Design of Highly Active Analogues of the Pyrrolo[1,2-*a*]benzimidazole Antitumor Agents

William A. Craigo, Benjamin W. LeSueur, and Edward B. Skibo*

Department of Chemistry and Biochemistry, Arizona State University, Tempe, Arizona 85287-1604

The pyrrolo[1,2-*a*]benzimidazole (PBI) reductive alkylating agents have been investigated in this laboratory since their discovery in the late 1980s. Of all the structural modifications of the PBIs investigated so far, the variation of the 3-substituent has the greatest influence on cytotoxicity, toxicity, and in vivo antitumor activity. In the present study, we prepared both the *R* and *S* enantiomers of nitrogen-containing 3-substituents possessing hydrogen-bonding capability as well as varying basicity. The rationale was to take advantage of stereoselective DT-diaphorase reductive activation as well as hydrogen bonding in the DNA major groove. As a result of these studies, analogues were discovered possessing among the highest hollow fiber tumor assay scores observed in hundreds of natural and synthetic antitumor agents. Our findings indicate that a relatively basic 3-substituent is required for outstanding PBI cytotoxicity but that the importance of using pure enantiomers is still open to study.

Introduction

Work in this laboratory[1−4] has been involved in the design of a new class of DNA cleaving agent based on the pyrrolo[1,2-*a*]benzimidazole (PBI) ring system. These agents were designed to alkylate the phosphate backbone upon DT-diaphorase-mediated reduction resulting in a hydrolytically labile phosphotriester; the reductive activation to the hydroquinone form is shown in the inset of Chart 1. While in the hydroquinone form, these agents can hydrogen-bond to the major groove and thereby recognize base pairs.[5] As expected, the PBIs possess outstanding antitumor activity by virtue of their ability to cleave DNA upon reductive alkylation. In the past, we have investigated the influence of PBI structural modifications on cytotoxicity. Thus the fused pyrrolo ring,[6] the benzimidazole ring system,[6] the position of the aziridine ring substituent,[6] the 7-methyl substituent,[7] and the 3-substituent[8] have all been varied and correlated with cytotoxicity. The 3-substituent appears to be the most important determinant of antitumor activity and cytotoxicity, with LC$_{50}$ values varying by orders of magnitude as this substituent is varied. Indeed, previous studies showed that the chirality of the 3-substituent is important with respect to both bioactivation by DT-diaphorase and the interaction with DNA.[5] At the outset of the present study, we postulated that both the hydrogen-bonding capability of the 3-substituent and the configuration of the 3-stereocenter could influence the substrate specificity for DT-diaphorase as well as the alkylation of DNA. Previous studies showed that the presence of a carbamate residue at the 3-position greatly increased the alkylation of DNA, presumably as a result of hydrogen bonding in the major groove.[1,2,8]

Therefore we prepared and studied the enantiomers of the 3-substituted PBIs **1−3** shown in Chart 1. This study showed that *R*(+)- and *S*(−)-**1** and its racemic form possess outstanding activity in the National Cancer Institute's in vivo hollow fiber assay.[9] In fact, these

Chart 1
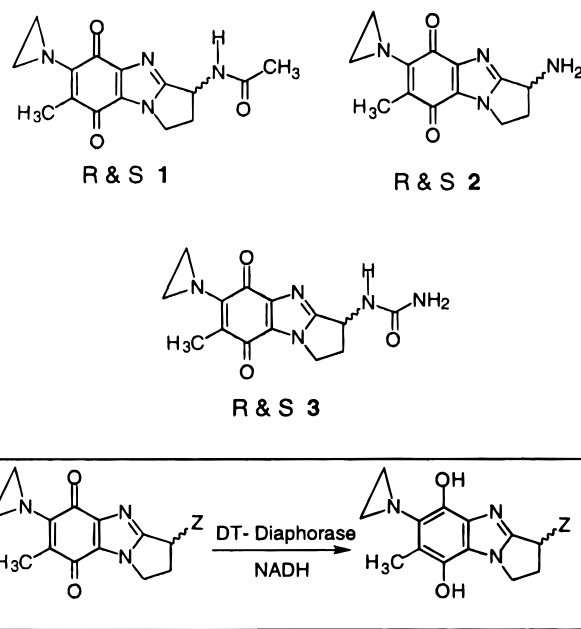
compounds are one of the most active among the hundreds of natural and synthetic agents screened in this assay. Compound *S*(−)-**2** is both highly cytotoxic and selective possessing LC$_{50}$ values $< 10^{-8}$ against some cancer lines and LC$_{50}$ values $> 10^{-4}$ against other lines. To follow is a description of the unambiguous synthesis of the enantiomers of **1−3**, their cytotoxicity and in vivo activity, measurements of their substrate specificity for DT-diaphorase, and finally their percent incorporation into DNA.

Synthesis

The preparation of the new PBIs is outlined in Schemes 1 and 2. Previous synthetic studies led to the preparation of racemic **4** employing 3-bromo-4-nitro-toluene and either racemic or *S*(−)-2,4-diaminobutanoic

Scheme 1
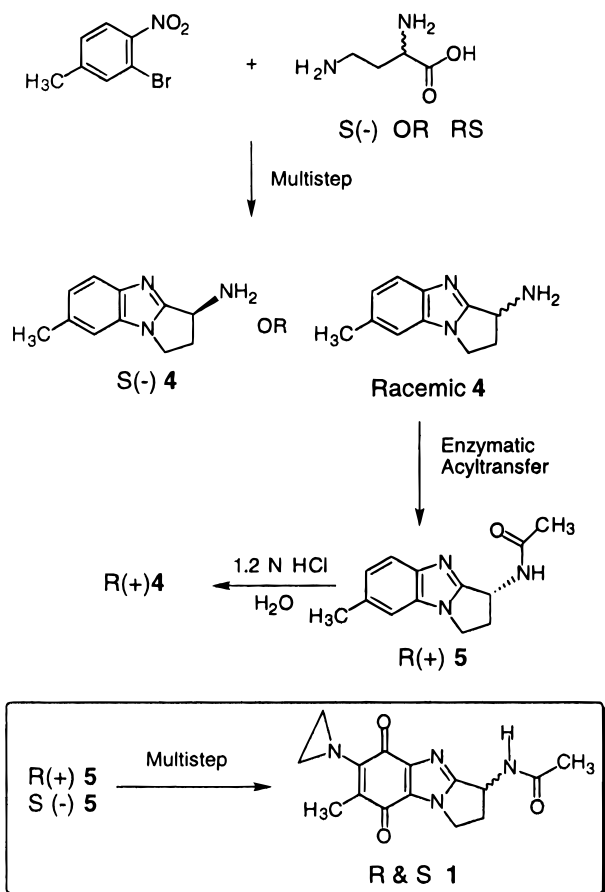
Scheme 2

acid.[4,5,10] Acetylation of $S(-)$-**4** to $S(-)$-**5** was followed by conversion to $S(-)$-**1**, Scheme 1. The previously unknown $R(+)$ enantiomer was prepared from racemic **4** employing an acyltransferase (ALTUS 20 CLEC catalyst), which afforded $R(+)$-**5** as the major product. Altus Inc. provides a kit of 40 acyltransferases to screen for enantiomeric excesses; only the mentioned acyltransferase gave a suitable result. Conversion of $R(+)$-**5** to the $R(+)$-**1** was carried out as previously described.[5]

To prepare the $R(+)$ or $S(-)$ forms of **2** and **3**, the $R(+)$ or $S(-)$ forms of **4** were trifluoroacetylated to afford **7**, Scheme 2. The trifluoroacetyl group was easily removed after the bromination and nitration reactions to afford the common intermediate **9**. PBI **2** was prepared from **9** by reduction, Fremy oxidation, and finally aziridination as previously described for the PBIs.[10] The same procedure was employed to convert the 3-carbamido derivative **10** to the PBI **2**.

In Vivo and In Vitro Screening Results

In vivo screening results of $S(-)$- and racemic **1**, employing the relatively new hollow fiber assay,[11] are discussed in conjunction with Table 1 and Figure 1.
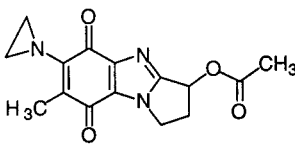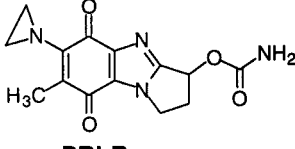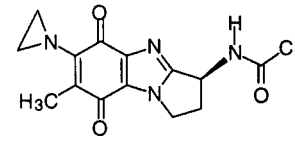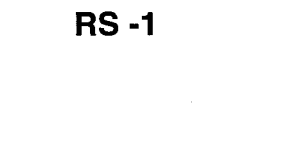
Hollow fiber assays were carried out in the following way. Human tumor cells are cultivated in polyvinylidene fluoride hollow fibers, and a sample of each cell line is implanted into each of two physiological compartments (intraperitoneally and subcutaneously). Mice are treated with either a high or a low dose using a qd × 4 schedule (four daily treatments) administered intraperitoneally. Altogether, 12 cell lines are studied resulting in 48 possible test combinations (12 cell lines
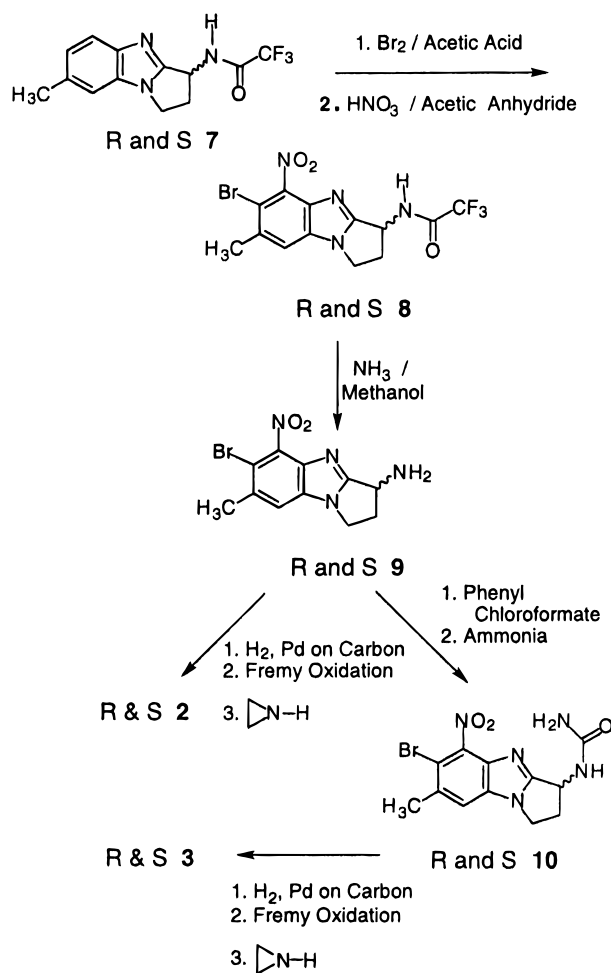
× 2 sites × 2 doses). A score of 2 is given to each test in which there is a % T/C of 50 or less (tumor mass 50% or less than the control). Thus the highest possible score is 96, but the typical score is only 5, and the highest score achieved so far is 64. The score is broken down into an intraperitoneal (ip) and a subcutaneaous (sc) score. A good sc score (≥8) indicates that the drug is able to get to the tumor site (subcutaneous) from a distant site (intraperitoneal) of injection. Both PBI-A and PBI-B shown in Table 1 are active in the hollow fiber assay and are active against melanoma, NSC lung cancer, breast cancer, and ovarian cancer. The 3-substituent of the PBI apparently is crucial for cytotoxic activity but is not required for the actual reductive alkylation process, which only requires the aziridinylquinone. Thus 3-unsubstituted PBI and the 3-hydroxy PBI are devoid of activity, while the lipophilic 3-propanoate derivative showed animal toxicity (100% drug deaths) at doses as low as 5 mg/kg without any significant antitumor activity.[8,3,4] The acetate and the carbamate, PBI-A and PBI-B, respectively, appear to have a suitable balance of polarity and lipophilicity in the 3-substituent for antitumor activity. These findings prompted the investigation of **1**, which bears a nitrogen instead of an oxygen bound to the 3-position. The data in Table 1 shows that both $S(-)$-**1** and RS-**1** have a higher score than PBI-A and -B. The high sc score of 14 for $S(-)$-**1** indicated that this agent can kill cancer cells at a location distant from the site of injection. However,

Table 1

	Intraperitonal Score	Subcutaneous Score	Total Score
PBI-A	40	8	48
PBI-B	24	6	30
S(-)-1	38	14	52
RS -1	46	6	52

Cancer cell line types sensitive to the PBIs:
  Melanoma
  Non-Small Cell Lung Cancer
  Breast Cancer
  Ovarian Cancer

Cancer cell line types sensitive to 1:
  Non-Small Cell Lung Cancer
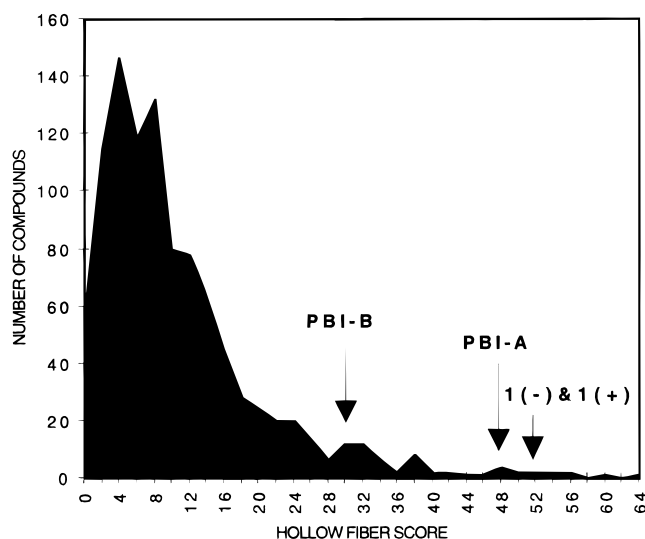 **CNS Cancer**
  Ovarian Cancer

Figure 1. Plot of the number of compounds studied at the National Cancer Institute versus their hollow fiber score. Development of the PBI analogues in this laboratory has resulted in lower scores in the hollow fiber assay.

the racemic form of **1** shows a lower sc score with a higher ip score suggesting that $R(+)$-**1** is less active at distant locations in this assay. Perhaps the $R(+)$ enantiomer is more susceptible to metabolic inactivation than the $S(-)$ enantiomer. Studies of both enantiomers, side by side, against a syngeneic tumor implant seem to suggest equivalent activity, Figure 2.

The National Cancer Institute has tested hundreds of new synthetic and natural products in the hollow fiber screen.[9] Among these compounds are PBI-A, PBI-B, $S(-)$-**1**, and RS-**1** whose rankings are shown in Figure 1 (the $R(+)$ analogue of **1** is currently being screened by the NCI). The typical antitumor agent only has a hollow fiber score of ~5, while $S(-)$-**1** and RS-**1** both score at 52 making them among the most active compounds studied by the National Cancer Institute.

Close inspection of Figure 1 shows that there are a few compounds with higher scores than $S(-)$-**1** and RS-**1**, the highest score being 64 for a natural product. Many of these compounds are too toxic and do not show activity against tumor implants. Indeed, the hollow fiber assay is not equivalent to drug assays against tumor implants, where angiogenesis metastases can intervene. Conversely, all compounds showing high activity against tumor implants are active in the hollow fiber assay.[9]

Examples of compounds showing higher hollow fiber scores than the PBIs are the natural products roridin A and flavopiridol, both of which are shown in Chart 2 along with their National Cancer Institute numbers. Roridin A did not perform well in human xenograft
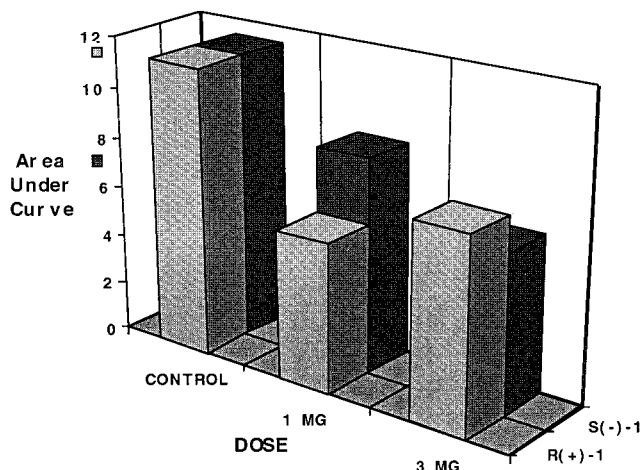
Figure 2. Results of S(−)-**1** and R(+)-**1** in the B-16 melanoma model in C57/bl mice (run at University of Arizona Cancer Center). These compounds were studied at two dose levels: 1 and 3 mg/kg ip on days 1, 5, and 9 after tumor implantation into the front flank muscle. Shown in the bar graph below is the area under the tumor versus time curve plotted against dose for each enantiomer. Note that there are no apparent differences between the enantiomers in these data.

Chart 2
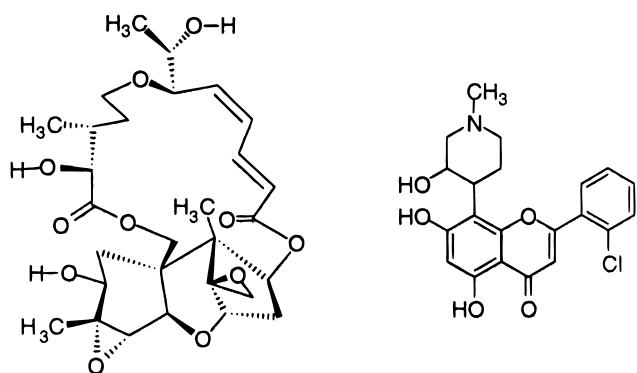
NSC 327993 (Roridin A)   NSC 649890 (Flavopiridol)

assays, while the cyclin-dependent kinase inhibitor[12] flavopiridol has activity and may show clinical promise.[13]

To determine if the PBIs $R(+)$- and $S(−)$-**1** will possess in vivo activity, assays employing syngeneic tumor implants (B-16 melanoma in C57/bl mice) were carried out as described below. The results of these studies with $R(+)$- and $S(−)$-**1**, Figure 2, failed to show much difference in activity between the enantiomers. Both $S(−)$- and $R(+)$-**1** did show large reductions in tumor mass with time, as measured from the area under the tumor mass versus time curve (AUC). In the syngeneic tumor graft assay, the tumor implant is in the front flank with ip drug injection, analogous to the sc implants of the hollow fiber assay. The activity of **1** in this assay is encouraging since a high hollow fiber assay score often can translate to high toxicity or inactivity in the in vivo assay.

In order to assess the influence of the 3-substituent configuration, the cytotoxicity of $R(+)$- and $S(−)$-**1** against a variety of cancers is compared in Figure 3. Each cancer type has a −log LC$_{50}$ value for each enantiomer, which is the average of two assays against
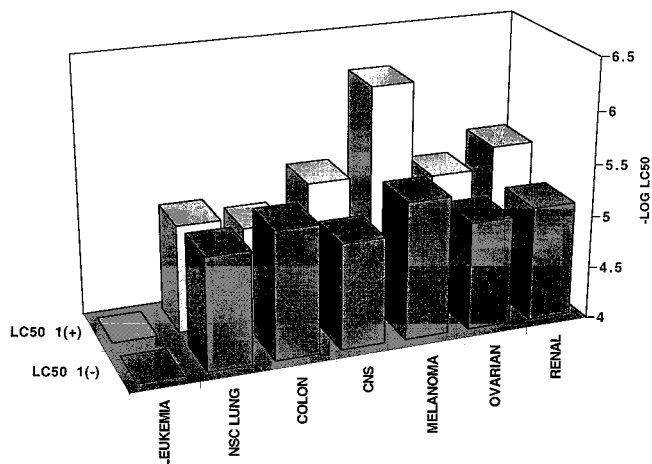

Figure 3. Plots of −log LC$_{50}$ versus cancer type for $R(+)$-**1** and $S(−)$-**1**. Each cancer type represents the average of 6−8 different cancer cell lines. The (+) enantiomer is much more active against melanoma, renal, ovarian, and CNS cancer cell lines, but this trend is reversed in colon cancer cell lines.
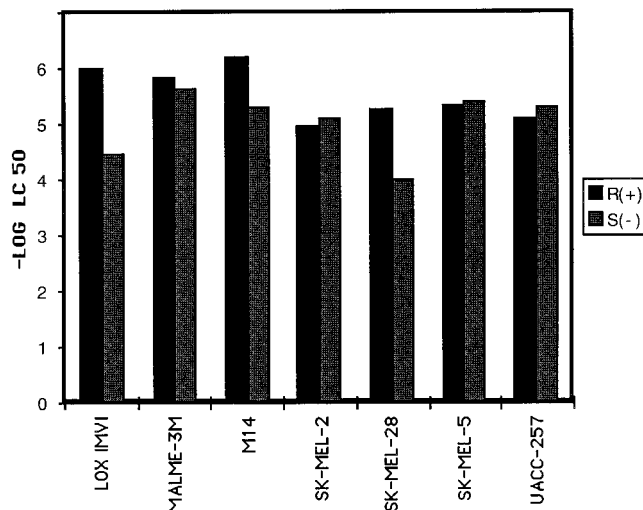

Figure 4. Plots of −log LC$_{50}$ versus melanoma cell line for $R(+)$-**1** and $S(−)$-**1**. Each −log LC$_{50}$ value is the average of two assays. Note that the enantiomeric differences reside in only a few cell lines.

a panel consisting of 6−8 human cancer cell lines. Therefore each −log LC$_{50}$ value is the average of 12−16 values. The identity of these cell lines and the assay methodology have been published.[14,15] Inspection of Figure 3 reveals that the $S(−)$-**1** is less active than the $R(+)$ enantiomer in melanoma, ovarian, non-small-cell lung, and renal cancers, but the trend is reversed in CNS cancers.

The other cancers have nearly the same average −log LC$_{50}$ values for each enantiomer. The enantiomeric differences in cytotoxicity reside in only a few of the cancers when individual cancer cell lines in the melanoma panel are compared, Figure 4. The origin of the enantiomeric differences may be due to the substrate specificity for DT-diaphorase or enantioselective reactions with DNA, both of which are discussed in the following two sections of this report.

Besides studying the influence of stereochemistry, we also varied the hydrogen-bonding capabilities of the 3-substituent. The properties of the 3-substituent are crucial for antitumor activity with low toxicity. Figure
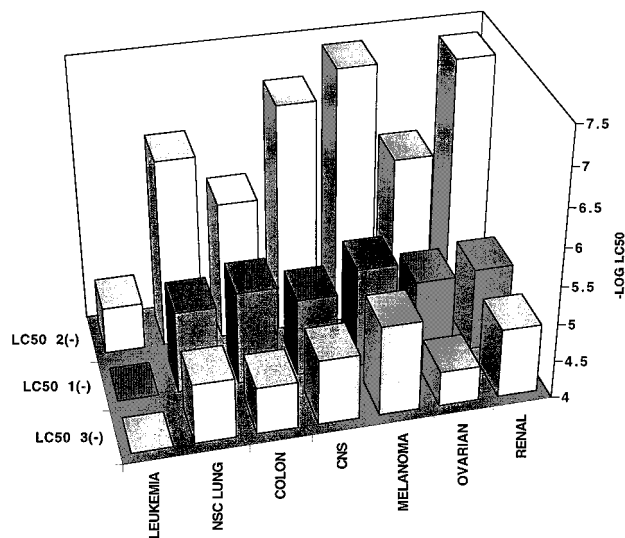
Figure 5. Plots of $-\log \mathrm{LC}_{50}$ versus cancer type for $S(-)$-**1**, **2**, and **3**. Each cancer type represents the average of $6-8$ different cancer cell lines. The 3-amino derivative **2** shows high cytotoxicity against non-small-cell lung, CNS, melanoma, ovarian, and renal cancers.

1 shows the increasing activity in the hollow fiber assay as the 3-substituent is changed from carbamate (PBI-B), to acetate (PBI-A), and finally to the 3-acetamido (**1**) substituent. When the 3-hydroxy group is changed to 3-amino (**2**), there is nearly a millionfold change in cytotoxicity (the 3-hydroxy analogue is noncytotoxic with LC_{50} values $> 10^{-4}$, while the 3-amino analogue is very cytotoxic with LC_{50} values in the nanomolar range in some cell lines). This finding suggests that a basic group in the 3-position is required for cytotoxicity because the large difference in cytotoxicity seems to reflect the relative pK_a values of a protonated amine versus a protonated alcohol.

Figure 5 contrasts the relative cytotoxicities of the $S(-)$ forms of **1**−**3** against several types of cancer. Preliminary studies indicate that the 3-amino substituent greatly enhances the alkylation of DNA, perhaps explaining the high cytotoxicity. At the present time we are carrying out in vivo studies of **2** to determine if the high cytotoxicity translates to antitumor activity or toxicity.

DT-Diaphorase Substrate Activity

The enantiomeric differences in cytotoxicity illustrated in Figures 3 and 4 could have their origin in the substrate specificity of DT-diaphorase. This enzyme can activate antitumor agents by two-electron reduction in both normal and cancerous tissues.[16,17] Some cancer cells can be sensitive to a reductive alkylating agent by virtue of high levels of DT-diaphorase[18] or a high substrate specificity. Recent studies have shown that there is a direct correlation between the substrate activity for DT-diaphorase and cytotoxicity.[19] Our earlier PBIs, as well as **1**−**3**, show a high correlation with the concentration of DT-diaphorase in cancer cells.[8] The correlation coefficients are in the $0.6-0.7$ range, but never higher. Perhaps the heterogeneous structure of DT-diaphorase could be responsible for the absence of a high correlation coefficient. Thus, a low substrate specificity of the PBI for the cell's DT-diaphorase would diminish the correlation with the enzyme's concentration.
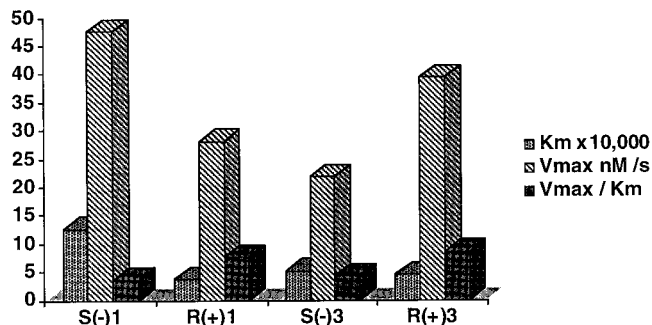

Figure 6. K_m, V_{max}, and V_{max}/K_m parameters obtained for the enantiomers of **1** and **3** with purified rat liver DT-diaphorase. The V_{max}/K_m value is a measure of the relative specificity of these substrates for the enzyme.

Depending on the organ and species source, the substrate and inhibition properties of DT-diaphorase can vary widely.[18,20] The structure of the enzyme even varies by ethnic origin, which may be a factor in the success of cancer chemotherapy in some patients.[21] Since the structure of DT-diaphorase varies by organ system, the enzyme could also vary by the organ system cancer. Thus cancers originating from these organs (lung, renal, ovarian, etc.) will a possess slightly different DT-diaphorase, assuming some degree of differentiation. Our previous studies indicated that the bulk of the 3-substituent and its stereochemistry[5] influence the substrate specificity of DT-diaphorase.

In the present study both the stereochemistry and the hydrogen-bonding capabilities of the 3-substituent (Chart 1) were varied to assess their influence on DT-diaphorase substrate specificity and cancer selectivity. The K_m, V_{max}, and V_{max}/K_m parameters for both enantiomers of **1** and **3** are provided in Figure 6. For both **1** and **3**, the DT-diaphorase has a 2-fold higher specificity for the $R(+)$ enantiomer than the $S(-)$ enantiomer. This observation could explain the higher cytotoxicity of the $R(+)$ enantiomer against some cancer panels, Figures 3 and 4. However, the heterogeneity of the enzyme could either reverse this trend or result in equal cytotoxicity for the enantiomers in other cancer panels.

Validation of the concept of differential antitumor activity based on differential DT-diaphorase specificity will rely on the isolation and characterization of the DT-diaphorase substrate specificity from a series of human cancer cell lines. Since only one human cancer DT-diaphorase has been cloned so far,[22] validation of this concept will be a slow process.

DNA Reductive Alkylation

Once the PBI is reductively activated in a specific cancer cell, cytotoxicity would result from the efficient alkylation of DNA by the reduced species. The work in this laboratory has validated the major groove binding model,[2,3] wherein the reduced PBI binds to the DNA major groove in a preequilibrium step followed by phosphate alkylation,[1,2] Chart 3. Although rigorous evidence of major groove binding is still lacking, the model has been employed in the design of efficient DNA cleaving agents. Presumably, the structure and stereochemistry of the 3-substituent greatly influences the degree of DNA alkylation by hydrogen bonding in the major groove.[2,3,7,8] For example, the reduced carbamate derivative PBI-B interacts predominately at A-T base
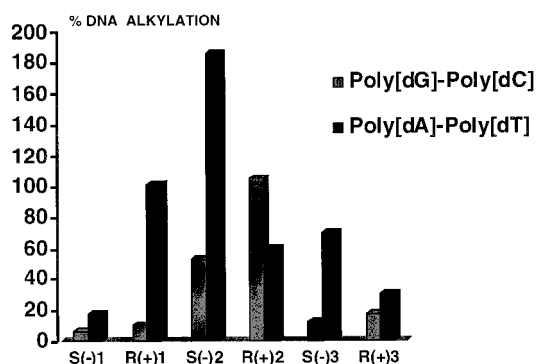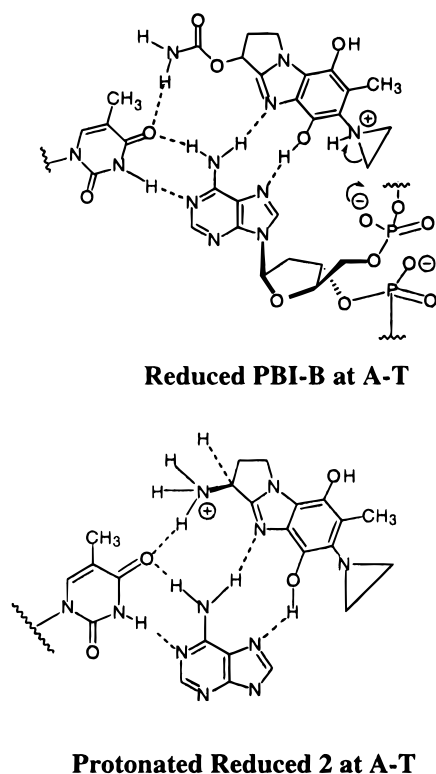
Chart 3

Reduced PBI-B at A-T

Protonated Reduced 2 at A-T

Figure 7. Bar graph of percent DNA base pair reductive alkylation of poly(dG)·poly(dC) and poly(dA)·poly(dT) by the enantiomers of **1**−**3**.

pairs presumably due to hydrogen bonding of the carbamate amine group with the thymine carbonyl,[2] Chart 3.

Found in Figure 7 is the percent base pair alkylation of DNA homopolymers obtained with the reduced enantiomers of **1**−**3**. PBI alkylation of DNA followed by air oxidation affords the blue-colored aminoquinone (blue DNA), permitting an easy quantitation of alkylation employing UV−vis spectroscopy (see Experimental Section).[2] The percent alkylation is based on the number of alkylations per base pair: all base pairs alkylated once is 100%, and two alkylations per base pair is 200%.

The data in Figure 7 indicate that the 3-substituents of **1**−**3** in most cases favor A-T over G-C alkylation. The 3-amino derivative **2** is a highly efficient reductive alkylating agent of DNA and it can alkylate up to 2 times per base pair (200%) upon reductive activation. This alkylated DNA is insoluble in all solvents except hot DMSO and therefore difficult to work with. The reason for the overalkylation by reduced **2** may be the

protonation of the amino group and better hydrogen bonding in the major groove as illustrated in Chart 3, or perhaps an electrostatic interaction between the positive nitrogen center and the phosphate backbone. The data in Figure 7 also show enantiomeric differences in reductive alkylation percent values. Since we used homopolymeric DNA, rather than alternating polymers, the 3-substituent will point in the 3′- or 5′-direction depending on the enantiomer employed. Differing hydrogen-bonding interactions will result in a variable percent alkylation and even alter base pair specificity, as in the case of $R(+)$-**2**. The differential cytotoxicity of enantiomers (Figures 3 and 4) probably does not originate with DNA base pair recognition, although we are investigating this possibility further. The site(s) of DNA alkylation by reduced **1**−**3** is currently under investigation, although phosphate alkylation is likely based on our experience with the PBIs.

Uniqueness of the PBIs

The differences between the clinically used aziridinyl compounds and the PBIs were apparent from COMPARE correlations[8] as well as from previously reported mechanistic studies.[1,2] COMPARE was developed at the NCI to compare the patterns of cytotoxicity in 60-cell line cancer screens.[14] Antitumor agents with identical mechanisms of action possess identical or nearly identical cytotoxicity patterns (correlation coefficient > 0.8). For example, anthracycline analogues (doxorubicin, rubidazone, daunamycin) have a high correlation (>0.9) with each other as do the DNA alkylating agents (chlorambucil, thiotepa, triethylenemelamine). In contrast, the cytotoxicity pattern of the PBIs does not correlate highly with those of any known antitumor agent. Shown in Chart 4 are antitumor agents with the highest correlation coefficients with $S(-)$-**1** and $R(+)$-**1** out of ∼20 000 compounds in the NCI's archives. The magnitude of the correlation coefficients in Chart 4 suggests some overlay in cytotoxicity mechanism with the PBIs. Like the PBIs, triethylenemelamine alkylates DNA,[23] while tetrocarcin A interferes with DNA synthesis.[24,25] The overall uniqueness of the PBIs probably originates with their substrate specificity for DT-diaphorase and DNA alkylation mechanism (major groove binding and phosphate alkylation as opposed to N-7 alkylation).

Conclusions

The previously studied PBIs bear an oxygen substituent at the 3-position, usually attached to an ester or carbamate group. These PBIs showed good antitumor activity, which prompted structure−activity studies over the years.[3,4] The present study shows that the placement of a nitrogen at the 3-position, either as an amine, carbamido, or amide, results in a more active PBI with respect to both cytotoxicity and antitumor activity. The reason for the enhanced cytotoxicity/antitumor activity appears to be the efficient reductive alkylation of DNA brought about by a relatively basic 3-substituent. For example the 3-amino analogue **2** can reductively alkylate DNA up to 2 times per base pair when present in excess. The importance of the 3-substituent basicity is well-illustrated by comparing the cytotoxicity of the 3-hydroxy and 3-amino PBIs: the 3-hydroxy substituent has LC_{50} values > 10^{-4}, while the 3-amino PBI has LC_{50}

Chart 4
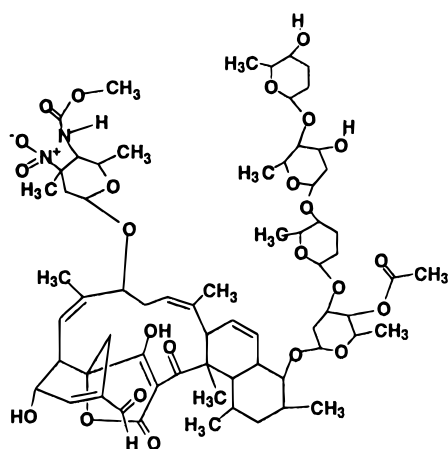
TETROCARCIN-A
NSC 333856
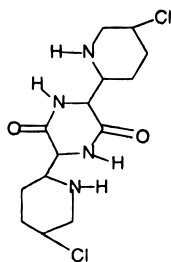0.641 CORRELATION COEFFICIENT
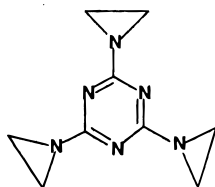
TRIETHYLENEMELAMINE
NSC 9706
0.713 CORRELATION COEFFICIENT

PIPERAZINEDIONE
NSC 135758
0.718 CORRELATION COEFFICIENT

values < 10^{-8} in human cancer cell lines. A conclusion regarding the better enantiomer for antitumor studies has not been reached, although the $R(+)$ enantiomer seems to be more active than the $S(-)$ enantiomer against some cancer panels. The greater activity of the $R(+)$ enantiomer may stem from its higher substrate specificity for DT-diaphorase. Further in vivo antitumor and toxicity studies with **1**−**3** should determine which is the better enantiomer for clinical trials.

Experimental Section

All solutions and buffers for kinetic, DNA, and electrophoresis studies used doubly distilled water. All analytically pure compounds were dried under high vacuum in a drying pistol over refluxing toluene. Elemental analyses were run at Atlantic Microlab, Inc., Norcross, GA. All TLCs were performed on silica gel plates using a variety of solvents and a fluorescent indicator for visualization. IR spectra were taken as thin films and the strongest absorbances reported. ^{1}H NMR spectra were obtained from a 300-MHz spectrometer. All chemical shifts are reported relative to TMS. Optical rotations were obtained from a Perkin-Elmer polarimeter employing a 10-cm quartz cell, 0.2 g/dL enantiomer in methanol. Enantiomeric purity was determined using optical rotations and chiral HPLC (see Chiral High-Pressure Liquid Chromatography). Intermediates leading to the pure enantiomers of **1**−**3** were characterized by their rotation of plane-polarized light (sodium D-line) and/or chiral HPLC. The final products **1**−**3** did not show clear rotation of the sodium D-line, and comfirmation of enantiomeric purity was made by chiral HPLC; all products were >99% enantiomerically pure. The syntheses of new compounds are outlined below.

(**R**)-(+)-3-Trifluoroacetamido-2,3-dihydro-7-methyl-1*H*-pyrrolo[1,2-*a*]benzimidazole (*R*(+)-7) was prepared from racemic **4** by the following three-step process. To 543 mg (2.9 mmol) of racemic **4** in a 250-mL round-bottom flask was added 310 mg of ALTUS 20 CLEC catalyst along with 104 mL of ethyl acetate. The resulting mixture was stirred vigorously for 30 min, and solids were filtered off and washed 3× with 10-mL portions of CHCl$_3$. The extraction solvent was removed under reduced pressure to afford a residue, which was placed on a silica gel column employing 3% methanol in chloroform as the eluent. Pure $R(+)$-**5** eluted from the column as the first band. The product was recrystallized from ethyl acetate/hexane: 244 mg (37%) yield; mp 219−220 °C; TLC (chloroform/methanol [90:10]) $R_f = 0.38$; IR (KBr pellet) 3245, 3068, 2990, 1635, 1560, 1420 cm^{-1}; ^{1}H NMR (CDCl$_3$) δ 7.75 (1H, s, acetamido proton) 7.47 (1H, d, $J = 8.4$ Hz, 5-aromatic proton), 7.02 (1H, d, $J = 8.4$ Hz, 6-aromatic proton), 6.88 (1H, s, 8-aromatic proton), 5.41 (1H, m, 3-methine proton), 4.0−3.8 (2H, m, 1-methylene protons), 3.25−3.15 (1H, m, 2-methylene proton), 2.55−2.39 (1H, m, 2-methylene proton) 2.43 (3H, s, methyl), 2.09 (3H, s, methyl); MS (EI) m/z 229 (M$^+$), 186 (M$^+$ − COCH$_3$), 171, 158, 145, 133, 116, 104. Rotations: $R(+)$ $[\alpha]^{25}_D$ = +104.4° (c = 0.41, MeOH).

The deacetylation of $R(+)$-**5** was carried out by dissolving 210 mg (0.877 mmol) in 12 mL of 1.2 N hydrochloric acid and refluxing the solution for 9 h. The solvent was removed under vacuum to afford a white solid, which was dissolved in water and then buffered to pH 7 with saturated sodium bicarbonate solution. The neutralized solution was extracted 5× with 30-mL portions of chloroform, and the extracts were dried over sodium sulfate. Concentration of the dried extracts and recrystallization from chloroform/hexane afforded 155 mg (95%) of $R(+)$-**4** as a white solid. Rotations: $R(+)$-**4** $[\alpha]^{25}_D$ = +20.9° (c = 1.1, MeOH) and $S(-)$-**4** $[\alpha]^{25}_D$ = −20.7° (c = 0.2, MeOH).

Trifluoroacetylation of $R(+)$-**4** was carried out by dissolving 155 mg (0.83 mmol) in 3 mL of trifluoroacetic acid followed by addition of 3 mL of trifluoroacetic anhydride. The reaction mixture was stirred for 20 min at room temperature and then poured into 150 mL of 0.1 M pH 7.0 phosphate buffer. The resulting solution was extracted 3× with 20-mL portions of ethyl acetate, and the extracts were washed 2× with 10-mL portions of saturated sodium bicarbonate and then dried over sodium sulfate. The extracts were concentrated to a residue, which was recrystallized from ethyl acetate/hexane to afford 152 mg (65%) of $R(+)$-**7**. Rotation: $R(+)$ $[\alpha]^{25}_D$ = +101.2° (c = 0.55, MeOH).

(**S**)-(−)-3-Trifluoroacetamido-2,3-dihydro-7-methyl-1*H*-pyrrolo[1,2-*a*]benzimidazole (*S*(−)-7). A solution of 683 mg (3.05 mmol) of $S(-)$-**4** was prepared in 20 mL of trifluoroacetic acid. To this solution was added 20 mL of trifluoroacetic anhydride, and the reaction was stirred for 25 min at room temperature. The completed reaction was poured into 700 mL of 0.1 M pH 7.0 phosphate buffer. This solution was extracted 4× with 40-mL portions of ethyl acetate, and then the extracts were washed 3× with 20-mL portions of saturated aqueous bicarbonate solution and dried over Na$_2$SO$_4$. The solvent was removed under reduced pressure and the product recrystallized from ethyl acetate/hexane: 546 mg (63%) yield; mp 227−228 °C; TLC (chloroform/methanol [90:10]) $R_f = 0.68$; IR (KBr pellet) 3178, 2987, 2912, 2858, 1724, 1572, 1523, 1213, 1186, 1153 cm^{-1}; ^{1}H NMR (CDCl$_3$) δ 9.75 (1H, bs, −NH), 7.41 (1H,

d, J = 8.1 Hz, 5 − aromatic proton) 7.02 (1H, d, J = 8.1 Hz, 6-aromatic proton), 6.79 (1H, s, 8-aromatic proton), 5.43 (1H, q, J = 6.3 Hz, 3-methine proton), 4.08−3.89 (2H, m, 1-methylene proton), 3.31−3.89 (1H, m, 2-methylene proton), 2.69−2.58 (1H, m, 2-methylene proton), 2.41 (3H, s, 2-methyl protons); MS (EI mode) m/z 283 (M$^+$), 186 (M$^+$ − CF$_3$CO), 121, 131, 105. Rotation: S(−)-**7** [α]$^{25}_D$ = −108.7° (c = 0.42, MeOH). Anal. (C$_{13}$H$_{12}$F$_3$N$_3$O) C, H, N.

6-Bromo-3-trifluoroacetamido-2,3-dihydro-7-methyl-5-nitro-1*H*-pyrrolo[1,2-*a*]benzimidazole (8) was prepared by the following two-step procedure starting with **7**. To a solution of 500 mg (1.76 mmol) of **7** in 25 mL of acetic acid was added 0.25 mL of a solution of bromine 0.8 M in acetic acid. The resulting solution was stirred at room temperature for 20 min and then quenched by dilution with 500 mL of 0.1 M pH 7.0 phosphate buffer. The resulting mixture was extracted 3× with 80-mL portions of ethyl acetate, and then the extracts were washed 2× with 80-mL portions of saturated aqueous sodium bicarbonate solution. The extracts were dried over Na$_2$SO$_4$, and the solvent was removed under reduced pressure to afford the bromo derivative which was recrystallized from ethyl acetate/hexane: 546 mg (85%) yield; mp 215−217 °C; TLC (chloroform/methanol [90:10]) R_f = 0.50; IR (KBr pellet) 3178, 2984, 2859, 1730, 1570, 1522, 1445, 1221, 1186, 1148 cm^{-1}; ^{1}H NMR (CDCl$_3$) δ 9.9 (1H, bs, amide NH), 7.61 (1H, s, 5-aromatic proton), 6.83 (1H, s, 8-aromatic proton), 5.48−5.40 (1H, m, 3-methine proton), 4.17−3.95 (2H, m, 1-methylene protons), 3.33−3.26 (1H, m, 2-methylene proton), 2.77−2.65 (1H m, 2-methylene proton), 2.42 (3H, s, methyl); MS (EI) m/z 363 & 361 (M$^+$, ^{79}Br & ^{81}Br), 264 & 266 (M$^+$ − COCF$_3$), 223, 169, 130, 90. Rotations: R(+) [α]$^{25}_D$ = +92.6° (c = 0.47, MeOH); S(−) [α]$^{25}_D$ = −97.8° (c = 0.18, MeOH). Anal. (C$_{13}$H$_{11}$BrF$_3$N$_3$O) C, H, N.

To 12 mL of fuming nitric acid, cooled to 0 °C was slowly added 500 mg (1.4 mmol) of the bromo derivative with stirring. To the resulting solution was added 1.14 mL of acetic anhydride with continued stirring and cooling. After stirring at 0 °C for 5 min, the reaction mixture was allowed to come to room temperature and then stirred for 1.5 h. The completed reaction was poured into 450 mL of ice water and the mixture buffered to pH 7 with NaHCO$_3$. The product was extracted 3× with 50-mL portions of ethyl acetate. The extracts were then dried over Na$_2$SO$_4$, and solvent was removed to afford a yellow residue. Recrystallization from a minimum amount of ethyl acetate, facilitated by the addition of hexane, afforded **8** as light yellow crystals: 466 mg (89%) yield; mp 245−247 °C; TLC (chloroform/methanol [90:10]) R_f = 0.60; IR (KBr pellet) 3246, 3044, 1741, 1657, 1570, 1538, 1370, 1229, 1159 cm^{-1}; ^{1}H NMR (CDCl$_3$) δ 10.21 (1H, s, amide NH), 7.38 (1H, s, 8-aromatic proton), 4.75−4.70 (1H, m, 3-methine proton), 4.52−4.42 (1H, m, 1-methylene proton), 4.20−4.12 (1H, m, 1-methylene proton), 3.50−3.40 (1H, m, 2-methylene proton), 2.95−2.85 (1H, m, 2-methylene proton), 2.58 (3H, s, methyl); MS (EI) m/z 406 (M$^+$), 361 (M$^+$ − NO$_2$), 309, 293, 280, 263, 189. Rotations: R(+) [α]$^{25}_D$ = +70.12° (c = 0.42, MeOH); S(−) [α]$^{25}_D$ = − 64.0° (c = 0.39, MeOH). Anal. (C$_{13}$H$_{10}$BrF$_3$N$_4$O$_3$) C, H, N.

3-Amino-6-bromo-2,3-dihydro-7-methyl-5-nitro-1*H*-pyrrolo[1,2-*a*]benzimidazole (9). To a solution of 45 mL of methanol cooled to −70 °C in an 2-propanol/dry ice bath was bubbled gaseous ammonia until the volume of liquid doubled. To the resulting solution was added 300 mg (0.737 mmol) of **8**, and the mixture was then removed from the dry ice bath and stirred for 48 h at room temperature. The solvent was evaporated, and the residue was recrystallized from chloroform/hexane to afford light brown crystals: 151 mg (66%) yield; mp 145−148 °C; TLC (chloroform/methanol [80:20]) R_f = 0.22; IR (KBr pellet) 3389, 2924, 1532, 1458, 1381, 1294, 878 cm^{-1}; ^{1}H NMR (CDCl$_3$) δ 7.36 (1H, s, aromatic proton), 4.58 (1H, dd, J = 7.9 Hz, J = 6.6 Hz, 3-methine proton), 4.29−4.21 and 4.09−4.01 (2H, 2m, 1-methylene protons), 3.15−3.03 and 2.51−2.39 (2H, 2m, 2- methylene protons), 2.58 (3H, s, 7-methyl); MS (EI) m/z 310 and 312 (M$^+$, ^{79}Br & ^{81}Br), 293 and 295 (M$^+$ − NH$_3$), 263 and 265 (M$^+$ − NH$_3$ − NO). Rotations: R(−) [α]$^{25}_D$

= −8.1° (c = 0.42, MeOH); S(+) [α]$^{25}_D$ = 10.1° (c = 0.16, MeOH). Anal. (C$_{11}$H$_{11}$BrN$_4$O$_2$·0.25H$_2$O) C, H, N.

3-Amino-6-aziridinyl-2,3-dihydro-7-methyl-1*H*-pyrrolo-[1,2-*a*]benzimidazole-5,8-dione (2). A solution consisting of 70 mg (0.225 mmol) of **9**, 70 mg of 5% Pd on charcoal, and 70 mL of methanol was shaken under 50 psi H$_2$ for 24 h. The reaction mixture was filtered through Celite, evaporated to dryness, and then combined with a solution of 0.333 g KH$_2$-PO$_4$ in 30 mL of water. The resulting solution was combined with another solution consisting of 1.0 g of KH$_2$PO$_4$ and 0.700 g of Fremy salt in 50 mL of water. The reaction mixture was stirred at room temperature for 6 h and then concentrated under high vacuum to a residue, which was placed on a 25-mL Bakerbond phenyl reverse-phase column prepared with 100% water. The unstable aminoquinone was eluted from the column with water, and the combined fractions were concentrated to a dry residue, which was dissolved in 10 mL of methanol and 0.3 mL of aziridine. This reaction mixture was stirred at room temperature for 5 h. The solvent was evaporated, and the residue was purified by flash column chromatography employing chloroform/methanol [95:5] as the eluent. The product fractions were evaporated to dryness, and the residue was recrystallized from chloroform/hexane to afford **2** as a red solid: 6.0 mg (10.3%) overall yield; mp > 240 °C dec; TLC (chloroform/methanol [80:20]) R_f = 0.17; IR (KBr pellet) 3387, 2996, 2924, 1674, 1632, 1576, 1518, 1377, 1341, 1312, 1140, 988, cm^{-1}; ^{1}H NMR (DMSO−d_6) δ 4.23−4.15 and 4.06−3.97 (3H, 2m, 3-methine and 1-methylene), 2.89−2.78 and 2.27−2.16 (2H, 2m, 2-methylene), 2.29 (4H, s, aziridinyl protons), 1.94 (3H, s, 7−methyl); MS (EI) m/z 258 (M$^+$), 240, 214. Anal. (C$_{13}$H$_{14}$N$_4$O$_2$·0.25H$_2$O) C, H; N: calcd, 21.32; found, 20.30.

6-Bromo-3-carbamido-2,3-dihydro-7-methyl-5-nitro-1*H*-pyrrolo[1,2-*a*]benzimidazole (10) was prepared by the following two-step procedure starting with **9**. A solution of 150 mg (0.482 mmol) **9** in 9 mL of dry pyridine was cooled to 0 °C in an ice bath. To the cooled solution was added 0.3 mL of phenyl chloroformate, and the reaction mixture was stirred at 0 °C for 15 min. The mixture was then removed from the ice bath and allowed to warm to room temperature with stirring over 1 h. The reaction mixture was diluted with 50 mL of ethyl acetate and the resulting mixture washed 3× with 15 mL of 20% aqueous acetic acid, 2× with 10-mL portions of 0.12 N aqueous hydrochloric acid, and finally 2× with 15 mL of water. The ethyl acetate layer was dried over Na$_2$SO$_4$, and the solvent was evaporated to a residue, which was recrystallized from chloroform/hexane to afford the phenoxyamido derivative as a light brown solid: 162 mg (78%) yield; mp 175−178 °C; TLC (chloroform/methanol [80:20]) R_f = 0.66; IR (KBr pellet) 3306, 1736, 1537, 1491, 1208 cm^{-1}; ^{1}H NMR (DMSO-d_6) δ 8.55 (1H, d, J = 9 Hz, amide proton), 7.87 (1H, s, C(8) proton), 7.4−6.7 (5H, 3m, aromatic protons), 5.28 (1H, q, J = 6.6 Hz, 3-methine), 4.36−4.26 and 4.18−4.09 (2H, 2m, 1-methylene), 3.13−3.01 and 2.61−2.49 (2H, 2m, 2-methylene), 2.54 (3H, s, 7-methyl); MS (EI) m/z 430 and 432 (M$^+$, ^{79}Br & ^{81}Br). Rotations: R(−) [α]$^{25}_D$ = +13.6° (c = 0.26, MeOH); S(+) [α]$^{25}_D$ = −14.0° (c = 0.33, MeOH). Anal. (C$_{18}$H$_{15}$BrN$_4$O$_4$·0.25 H$_2$O) C, H, N.

Gaseous ammonia was passed into a dry flask cooled to −70 °C with 2-propanol/dry ice bath until 20 mL of liquid ammonia was obtained. A solution of 150 mg (0.348 mmol) of the phenoxyamido derivative in 10 mL of dry methylene chloride was added to the liquid ammonia, and the resulting mixture was stirred for 30 min at −70 °C. The reaction mixture was then removed from the dry ice bath and stirred for 3 h at room temperature. The solvent was evaporated, and the solid residue was recrystallized from chloroform/hexane to afford **10** as an off-white solid: 104 mg (84.5%) yield; mp 240−241 °C; TLC (chloroform/methanol [80:20]) R_f = 0.34; IR (KBr pellet) 3410, 3293, 2922, 1657, 1588, 1532, 1371 cm^{-1}; ^{1}H NMR (DMSO-d_6) δ 7.83 (1H, d, J = 1.2 Hz, aromatic proton), 6.69 (1H, d, J = 8.4 Hz, amide protons), 5.69 (2H, s, amide protons), 5.22 (1H, m, 3-methine), 4.30−4.21 and 4.11−4.03 (2H, 2m, 1-methylene), 2.99−2.88 and 2.41−2.30 (2H, 2m, 2-methylene),

2.54 (3H, s, 7-methyl); MS (EI) m/z 353 and 355 (M$^+$, ^{79}Br & ^{81}Br). Anal. (C$_{12}$H$_{12}$BrN$_5$O$_3$·0.5 H$_2$O) C, H, N.

3-Carbamido-6-aziridinyl-2,3-dihydro-7-methyl-1*H*-pyrrolo[1,2-*a*]benzimidazole-5,8-dione (3) was prepared from **10** by the following two-step procedure. A solution of 120 mg (0.339 mmol) of **10**, 80 mg of 5% Pd on charcoal, and 200 mL of methanol was shaken under 50 psi H$_2$ for 15 h. The reaction mixture was filtered through Celite, and the solvent was removed by evaporation. The residue was dissolved into a solution of 296 mg of KH$_2$PO$_4$ in 120 mL of water. To this solution was added a Fremy salt solution consisting of 1.2 g of Fremy salt and 1.8 g of KH$_2$PO$_4$ in 174 mL of water. The reaction was stirred at room temperature for 1.5 h and then concentrated with high vacuum. The residue was placed on a 25-mL Bakerbond phenyl reverse-phase column prepared with 100% water. The yellow product fractions were collected from the column employing water as the eluent. The fractions were evaporated to dryness, and the residue was recrystallized from ethyl acetate/hexane: 46 mg (52%) yield; mp 180−183 °C; TLC (chloroform/methanol [80:20]) R_f = 0.48; IR (KBr pellet) 3393, 3297, 3212, 1659, 1593, 1570, 1516, 1329, 1152 cm^{-1}; ^{1}H NMR (DMSO-d_6) δ 6.64 (1H, d, J = 8.4 Hz, amide proton), 6.57 (1H, d, J = 2.1 Hz, aromatic proton), 5.67 (2H, s, amine protons), 5.09-5.01 (1H, m, 3-methine), 4.29-4.21 and 4.14-4.06 (2H, 2m, 1-methylene), 2.99-2.88 and 2.41−230 (2H, 2m, 2-methylene), 2.01 (3H, d, J = 1.5 Hz, 7−methyl); MS (EI) m/z 260 (M$^+$), 243 (M$^+$ − NH$_3$), 217 (M$^+$ − H−N=C=O). Anal. (C$_{12}$H$_{12}$N$_4$O$_3$·0.35H$_2$O) C, H, N.

A solution of 20 mg (0.077 mmol) of the carbamide quinone, 10 mL of dry methanol, and 0.3 mL of aziridine was stirred at room temperature for 3 h. The reaction solvent was evaporated, and the red residue was dissolved into a 9:1 chloroform/methanol mixture and purified by flash column chromatography using 9:1 chloroform/methanol as the eluent. Evaporation of the solvent gave a red solid which was recrystallized from chloroform/hexane: 8.1 mg (35.0%) yield; mp 200−205 °C; TLC (chloroform/methanol [80:20]) R_f = 0.37; IR (KBr pellet) 3351, 1678, 1647, 1522, 1316, cm^{-1}; ^{1}H NMR (DMSO-d_6) δ 6.62 (1H, d, J = 7.8 Hz, amide proton), 5.65 (2H, s, amide protons), 5.04−4.96 (1H, m, 3−methine), 4.25−4.17 and 4.10−4.01 (2H, 2m, 1−methylene), 2.97−2.86 and 2.39−2.30 (2H, 2m, 2−methylene), 2.30 (4H, s, aziridinyl protons), 1.95 (3H, s, 7−methyl); MS (EI) m/z 301 (M$^+$). Anal. (C$_{14}$H$_{15}$N$_5$O$_3$·1.0H$_2$O) C, H; N: calcd, 21.90; found, 21.19.

Alkylation of DNA by Reduced PBIs. To a mixture of 1−2 mg of DNA (poly[dA]·poly[dT] or poly[dG]·poly[dC]) in 2.0 mL of 0.05 M pH 7.4 Tris buffer and 2 mg of Pd on carbon was added a 5:1 base-pair equivalent amount of the PBI dissolved in 0.5 mL of dimethyl sulfoxide. The resulting solution was degassed under argon for 30 min, after which the mixture was purged with H$_2$ for 10 min. The solution was then purged with argon for 10 min and placed in a 30 °C bath for 24 h. The reaction was opened to the air, and the catalyst was removed with a Millex-PF 0.8-μM syringe filter. The filtrate was adjusted to 0.3 M acetate with a 3 M stock solution of pH 5.1 acetate and the diluted with two volumes of ethanol. The mixture was chilled at −20 °C for 12 h and the DNA pellet collected by centrifuging at 12 000g for 20 min. The pellet was redissolved in water and then precipitated and centrifuged again. The resulting pellet was suspended in ethanol, centrifuged, and dried.

DT-Diaphorase Reduction Kinetics Studies. Rat liver DT-diaphorase was isolated as previously described.[5,26] Kinetic studies were carried out in 0.05 M pH 7.4 Tris·HCl buffer, under anaerobic conditions, employing Thunberg cuvettes. A 2 mM stock solution of the enantiomers of **1** and **2** was prepared in dimethyl sulfoxide. To the top port was added the quinone stock and to the bottom port was added DT-diaphorase and NADH in the Tris buffer. The top and bottom ports were purged with argon for 20 min and equilibrated to 30 °C. The ports were then mixed, and the reaction was followed at 296 nm for 25 min to obtain initial rates. The concentrations after mixing were 0.3 mM NADH, 1−20 × 10^{-5} M quinone, and 14.5 nM (based on flavin) of enzyme active sites. The value of $\Delta\epsilon$

was calculated from the initial and final absorbance values for complete quinone reduction; usual value for ϵ is 6000−8000 M^{-1} cm^{-1}. The value of $\Delta\epsilon$ was used to calculate V_{max} in M s^{-1}. The results were fitted to a Lineweaver−Burke plot from which V_{max}/K_m values were calculated.

Chiral High-Pressure Liquid Chromatography. All HPLC separations were performed on Chirex columns (50 × 3.2 mm) from Phenomenex. The detector was set at 287 nm and the sensitivity at 0.5. The flow rate was 0.1 mL/min, and the mobile phase consisted of hexane/1,2-dichloroethane/ethanol in a ratio of 60/30/10.

References

(1) Skibo, E. B.; Schulz, W. G. Pyrrolo[1,2-*a*]benzimidazole-Based Aziridinyl Quinones. A New Class of DNA Cleaving Agent Exhibiting G and A Base Specificity. *J. Med. Chem.* **1993**, *36*, 3050−3055.

(2) Schulz, W. G.; Nieman, R. A.; Skibo, E. B. Evidence for DNA Phosphate Backbone Alkylation and Cleavage by Pyrrolo[1,2-*a*]benzimidazoles, Small Molecules Capable of Causing Sequence Specific Phosphodiester Bond Hydrolysis. *Proc. Natl. Acad. Sci. U.S.A.* **1995**, *92*, 11854−11858.

(3) Skibo, E. B. The Discovery of the Pyrrolo[1,2-*a*]benzimidazole Antitumor Agents −The Design of Selective Antitumor Agents. *Curr. Med. Chem.* **1996**, *2*, 900−931.

(4) Skibo, E. B. Pyrrolobenzimidazoles in cancer treatment. *Exp. Opin. Ther. Patents.* **1998**, *8*, 673−701.

(5) Skibo, E. S.; Gordon, S.; Bess, L.; Boruah, R.; Heileman, J. Studies of Pyrrolo[1,2-*a*]benzimidazole Quinone DT-Diaphorase Substrate Activity, Topoisomerase II Inhibition Activity, and DNA Reductive Alkylation. *J. Med. Chem.* **1997**, *40*, 1327−1339.

(6) Skibo, E. B.; Islam, I.; Heileman, M. J.; Schulz, W. G. Structure−Activity Studies of Benzimidazole-Based DNA-Cleaving Agents. Comparison of Benzimidazole, Pyrrolobenzimidazole and Tetrahydropyridobenzimidazole Analogues. *J. Med. Chem.* **1994**, *37*, 78−92.

(7) Zhou, R.; Skibo, E. B. Chemistry of the Pyrrolo[1,2-*a*]benzimidazole Antitumor Agents: Influence of the 7-Substituent on the Ability to Alkylate DNA and Inhibit Topoisomerase II. *J. Med. Chem.* **1996**, *39*, 4321−4331.

(8) Schulz, W. G.; Islam, E.; Skibo, E. B. Pyrrolo[1,2-*a*]benzimidazole-Based Quinones and Iminoquinones. The Role of the 3-Substituent on Cytotoxicity. *J. Med. Chem.* **1995**, *38*, 109−118.

(9) Hollingshead, M.; Plowman, J.; Alley, M.; Mayo, J.; Sausville, E. Relevance of Tumor Models in Anticancer Drug Development. *Contributions to Oncology*; Krager Verlag: Germany, 1999.

(10) Skibo, E. B.; Islam, I.; Schulz, W. G.; Zhou, R.; Bess, L.; Boruah, R. The Organic Chemistry of the Pyrrolo[1,2-*a*]benzimidazole Antitumor Agents. An Example of Rational Drug Design. *Synlett* **1996**, 297−309.

(11) Hollingshead, M. G.; Alley, M. C.; Camalier, R. F.; Abbott, B. J.; Mayo, J. G.; Malspeis, L.; Grever, M. R. *Life Sci.* **1995**, *27*, 131−141.

(12) Sedlacek, H. H.; Czech, J.; Naik, R.; Kaur, G.; Worland, P.; Losiewicz, M.; Parker, B.; Carlson, B.; Smith, A.; Senderowicz, A.; Sausville, E. Flavopiridol (L86 8275; NSC 649890), a new kinase inhibitor for tumor therapy. *Int. J. Oncol.* **1996**, *9*, 1143−1168.

(13) Schrump, D. S.; Matthews, W.; Chen, G. A.; Mixon, A.; Altorki, N. K. Flavopiridol Mediates Cell Cycle Arrest and Apoptosis in Esophageal Cancer Cells. *Clin. Cancer Res.* **1998**, *4*, 2885−2890.

(14) Paull, D. K.; Shoemaker, R. H.; Hodes, L.; Monks, A.; Scudiero, D. A.; Rubinstein, L.; Plowman, J.; Boyd, M. R. Display and Analysis of Differential Activity of Drugs Against Human Tumor Cell Lines: Development of Mean Graph and COMPARE Algorithm. *J. Natl. Cancer Inst.* **1989**, *81*, 1088−1092.

(15) Alvarez, M.; Robey, R.; Sandor, V.; Nishiyama, K.; Matsumoto, Y.; Paull, K.; Bates, S.; Fojo, T. Using the national cancer institute anticancer drug screen to assess the effect of mrp expression on drug sensitivity profiles. *Mol. Pharmacol.* **1998**, *54*, 802−814.

(16) Riley, R. J.; Workman, P. DT-diaphorase and Cancer Chemotherapy. *Biochem. Pharmacol.* **1992**, *43*, 1657−1669.

(17) Marin, A.; deCerain, A. L.; Hamilton, E.; Lewis, A. D.; MartinezPenuela, J. M.; Idoate, M. A.; Bello, J. DT-diaphorase and cytochrome B-5 reductase in human lung and breast tumours. *Br. J. Cancer* **1997**, *76*, 923−929.

(18) Rauth, A. M.; Goldberg, Z.; Misra, V. DT-diaphorase: Possible roles in cancer chemotherapy and carcinogenesis. *Oncol. Res.* **1997**, *9*, 339−349.

(19) Beall, H. D.; Winski, S.; Swann, E.; Hudnott, A. R.; Cotterill, A. S.; OSullivan, N.; Green, S. J.; Bien, R.; Siegel, D.; Ross, D.; Moody, C. J. Indolequinone antitumor agents: Correlation between quinone structure, rate of metabolism by recombinant human NAD(P)H: quinone oxidoreductase, and in vitro cytotoxicity. *J. Med. Chem.* **1998**, *41*, 4755−4766.

(20) Wu, K. B.; Knox, R.; Sun, X. Z.; Joseph, P.; Jaiswal, A. K.; Zhang, D.; Deng, P. S. K.; Chen, S. Catalytic properties of NAD(P)H: quinone oxidoreductase-2 (NQO2), a dihydronicotinamide riboside dependent oxidoreductase. *Arch. Biochem. Biophys.* **1997**, *347*, 221−228.

(21) Kelsey, K. T.; Ross, D.; Traver, R. D.; Christiani, D. C.; Zuo, Z. F.; Spitz, M. R.; Wang, M.; Xu, X.; Lee, B. K.; Schwartz, B. S.; Wiencke, J. K. Ethnic variation in the prevalence of a common NAD(P)H quinone oxidoreductase polymorphism and its implications for anti-cancer chemotherapy. *Br. J. Cancer* **1997**, *76*, 852−854.

(22) Beall, H. D.; Mulcahy, R. T.; Siegel, D.; Traver, R. D.; Gibson, N. W.; Ross, D. Metabolism of Bioreductive Antitumor Compounds by Purified Rat and Human DT-Diaphorase. *Cancer Res.* **1994**, *54*, 3196−3201.

(23) Reynolds, R. C. Aziridines. In *Cancer Chemotherapeutic Agents*; Foye, W. O., Ed.; American Chemical Society: Washington, DC, 1995; pp 187−197.

(24) Morimoto, M.; Fukui, M.; Ohkubo, S.; Tamaoki, T.; Tomita, F. Tetrocarcins, New Antitumor Antibiotics. 3. Antitumor Activity of Tetrocarcin A. *J. Antibiot. (Tokyo)* **1982**, *35*, 1033−1037.

(25) Tamaoki, T.; Kasai, M.; Shirahata, K.; Ohkubo, S.; Morimoto, M.; Mineura, K.; Ishii, S.; Tomita, F. Tetrocarcins, Novel Antitumor Antibiotics. II. Isolation, Characterization and Antitumor Activity. *J. Antibiot. (Tokyo)* **1980**, *33*, 946−950.

(26) Höjeberg, B.; Blomberg, K.; Stenberg, S.; Lind, C. Biospecific Adsorption of Hepatic DT-Diaphorase on Immobilized Dicoumarol. *Arch. Biochem. Biophys.* **1981**, *207*, 205−216.